Multi Strategy SA-PSO Identification and Model-Based eMPC Control*

Zixu Li *1[0009−0000−1553−5882], Jingyuan Li *2[0009−0003−0257−8623], Yuhui Huang *3[0009−0008−8515−723X], Yiran Li *4[0009−0008−1282−8821], and Bin Xin *5[0000−0001−9989−0418]

*School of Automation, Beijing Institute of Technology, Beijing, China
[1] E-mail: 1120211166@bit.edu.cn
[2] E-mail: 1120211166@bit.edu.cn
[3] E-mail: 1120211098@bit.edu.cn
[4] E-mail: Li_yiran@bit.edu.cn
[5] E-mail: brucebin@bit.edu.cn

Abstract. In this paper, the inverted pendulum is controlled by QUBE DC motor, and the motor inverted pendulum system is identified when the sinusoidal signal is input. However, there is a large error when the angle of the pendulum is pre-identified by N4SID algorithm. Therefore, this paper designs a multi strategy optimization simulated annealing particle swarm optimization algorithm(MSSA-PSO), which can accurately identify the complex system with sinusoidal input signal. In the identification experiments of sinusoidal signals with multiple frequencies and amplitudes, this paper found that the algorithm performs relatively best at a frequency of 8 rad/s. Moreover, at a frequency of 8 rad/s, the algorithm can quickly reduce the error to 1.69% within 100 generations. Finally, based on the hardware model identified by particle swarm optimization, this paper designs an explicit MPC(eMPC) controller to control the inverted pendulum, and tests the constraint processing and anti disturbance performance of the system under the voltage pulse interference with different duty cycles, which realizes the inverted pendulum balance and has robustness under the interference.

Keywords: Inverted pendulum · Simulated annealing · Particle swarm optimization · Constraint processing · MPC control .

1 Introduction

The inverted pendulum problem is one of the most important problems in control theory and has been studied excessively in control literatures [1]. Because of its instability and complex dynamic characteristics, the system becomes an ideal platform to test the effect of control algorithm. With the development of control theory, the system identification and control algorithm design of inverted pendulum system have become the research focus. However, the highly nonlinear

* Supported by organization BIT, these authors contribute equally.

and unstable characteristics of inverted pendulum put forward higher requirements for system identification technology, which requires more refined methods to accurately capture its dynamic behavior [2].

Many scholars have completed innovations in system identification and swing stabilization control based on QUBE-Servo 2, such as nonlinear parameter identification based on variational method based on this platform [3]; Stable rotary pendulum fuzzy control based on QUBE motor [4]; Reinforce learning control based on a data-efficient method [5]; Event driven methods that can identify and suppress disturbances based on the platform [6], etc.

Based on the fact that system identification can be transformed into parameter identification, particle swarm optimization algorithm is widely used because of its convergence and simplicity. For instance, power system [7], Impulse response system [8] and robotic system [9]. Similarly, particle swarm optimization algorithm is also widely used in the research of inverted pendulum system [10,11].

Model predictive control (MPC) is a modern optimization-based control method, also called receding horizon control [12]. MPC is efficient due to some intrinsic advantages: (i) direct consideration of state and input constraints; (ii) applicability to general nonlinear MIMO systems; (iii) optimization of general performance criteria [13]. MPC has been successfully applied in many fields, such as vehicle control [14] and robot control [15]. Previously, many researchers used MPC to deal with the constraints and control the inverted pendulum system. For instance, a time-varying model predictive control framework for uncertain and under-actuated mechanical systems is designed in [16]. In [17], the stability of soft-constrained MPC is addressed based on simulations of inverted pendulums. In addition, in the display MPC method proposed by [18], the problem of real-time control of MPC is solved, and a rigorous and fast MPC method is given.

In Section 2 of this paper, the mathematical model of QUBE motor inverted pendulum system is derived theoretically. Then in Section 3, the simulated annealing PSO identification algorithm and its optimization strategies are designed to identify the mathematical and physical model of inverted pendulum system; Finally, based on the identification results of inverted pendulum physical model in Section 3, the author realized the pendulum stabilization control and anti-interference experiment of inverted pendulum system based on explicit MPC(eMPC) Method in Section 4.

2 Inverted Pendulum Modeling

The rotating shaft of inverted pendulum system is connected to is driven by the QUBE-servo system. When the pendulum is vertically downward, the pendulum angle $\alpha = 0$, and increases positively with counterclockwise rotation. See Table 1 for system parameters.

The Lagrangian of the pendulum system is the total kinetic energy of the rotating arm and the rotating pendulum minus the total potential energy of the rotating arm and the rotating pendulum. The two generalized coordinates in the system are connecting rod angle θ and pendulum angle α . After several

Fig. 1: The QUBE-Servo2 inverted pendulum system

Table 1: QUBE-Servo System Parameter

Symbol	Quantity	Numerical Value
m_r	rotating arm mass	0.095 kg
L_r	rotating arm length	0.085 m
m_p	pendulum mass	0.024 kg
L_p	pendulum length	0.129 m

differential calculations and linearization of the nonlinear motion equation near the working point, the linear motion equation of the inverted pendulum is:

$$\begin{aligned}\ddot{\theta} = \frac{1}{J_T}[&-(\frac{1}{4}m_pL_p^2 + J_p)D_r\dot{\theta} + \frac{1}{2}m_pL_pL_rD_p\dot{\alpha} \\ &+ \frac{1}{4}m_p^2L_p^2L_rg\alpha + (\frac{1}{4}m_pL_p^2 + J_p)\tau]\end{aligned} \tag{1}$$

$$\begin{aligned}\ddot{\alpha} = \frac{1}{J_T}[&\frac{1}{2}m_pL_pL_rD_r\dot{\theta} - (m_pL_r^2 + J_r)D_p\dot{\alpha} \\ &- \frac{1}{2}m_pL_pg(m_pL_r^2 + J_r)\alpha - \frac{1}{2}m_pL_pL_r\tau]\end{aligned} \tag{2}$$

Where:

$$\begin{aligned}J_T &= J_pm_pL_r^2 + J_rJ_p + \frac{1}{4}J_rm_pL_p^2 \\ J_r &= \frac{1}{12}m_rL_r^2,\ J_p = \frac{1}{12}m_pL_p^2\end{aligned} \tag{3}$$

A continuous linear space state equation is established, where u is the control input (DC motor input torque). For a rotary pendulum system, the status and output are defined as:

$$x = \left[\theta\ \alpha\ \dot{\theta}\ \dot{\alpha}\right]^T$$
$$y = \left[\theta\ \alpha\right]^T \tag{4}$$

3 Identification Algorithm Design

Remove the load disc on the QUBE motor and place a single arm swing on the upper end of the motor.

The Simulink simulation model is built as follows, and the 0 port of HIL read encoder timebase is used to collect the motor angle θ data, use 1 port to collect swing rod angle α data.

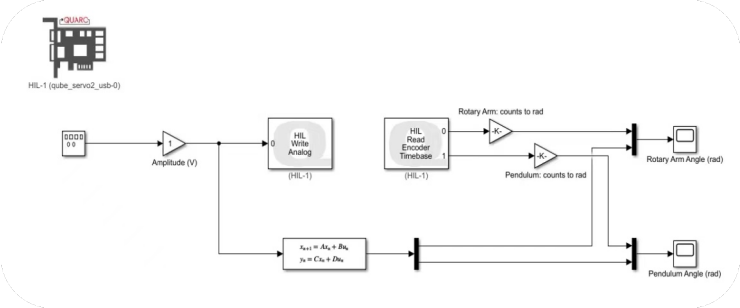

Fig. 2: Data acquisition model for Simulink simulation of inverted pendulum system

3.1 N4SID Pre-Identification

For pre-identification, this article wrote the N4SID code and adjust the algorithm parameters to make the identification of physical model data θ as accurate as possible. The identification of θ and α is shown in Fig.3.

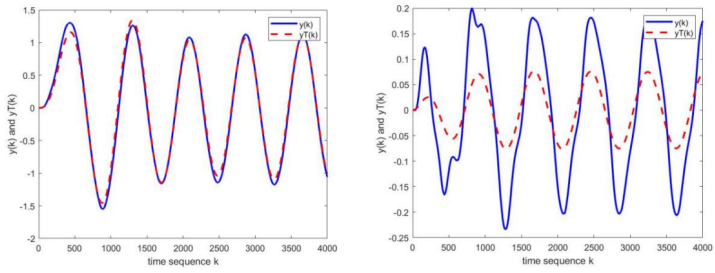

Fig. 3: Identification effect of N4SID on the physical model of inverted pendulum (left: θ; Right: α)

It can be seen that the N4SID method can be effectively implemented θ , but in fitting α there is a large deviation. Therefore, we need to design a more accurate algorithm to identify the system.

3.2 Adaptive SA-PSO identification algorithm

Different from the subspace method, the system identification of sinusoidal signal response data is regarded as an optimization problem, that is, to find the optimal estimation parameters. Based on this, the author designed an improved least square parameter estimation based on adaptive simulated annealing particle swarm optimization algorithm (SA-PSO) to identify the system.

Discretization and Data Processing Considering the discontinuity of sampling data, the original state space equation model is discretized. Discretization is replaced by the difference formula.After further arrangement, the least square form of the discrete model can be obtained.

$$\begin{bmatrix} V_m \\ V_m \end{bmatrix} = \begin{bmatrix} a_1 & a_2 & a_3 & a_4 & a_5 & 0 \\ a_6 & a_7 & 0 & a_8 & a_9 & a_{10} \end{bmatrix} \begin{bmatrix} \theta(k) \\ \theta(k+1) \\ \theta(k+2) \\ \alpha(k) \\ \alpha(k+1) \\ \alpha(k+2) \end{bmatrix} \tag{5}$$

The calculated theoretical values of each parameter are shown in Table 2.

Table 2: Theoretical Calculated Values of Parameters

a_1	a_2	a_3	a_4	a_5
4877.3	-9904.7	5027.4	46.416	-49.42
a_6	a_7	a_8	a_9	a_10
-150.1049	150.1049	-5179.4921	10250.7117	-5086.5424

Adaptive SA-PSO Algorithm Framework PSO algorithm starts from the random solution and finds the optimal solution through iteration; Evaluate the quality of solution by fitness. The basic parameters of PSO algorithm are shown in Table 4.

In the process of updating particle speed and position, in order to avoid falling into local optimal solution, random operators r_1 and r_2 are added to adjust (r_1 and r_2 are random numbers between 0 1). The generation formula of particle speed and position is as follows:

$$\begin{aligned} V_i^{kg+1} = \omega V_i^{kg} + c_1 r_1 (p_i^{kg} - X_i^{kg}) \\ + c_2 r_2 (BestS_i^{kg} - X_i^{kg}) \end{aligned} \tag{6}$$

Table 3: Basic Parameters of PSO Algorithm

G	Number of Iterations
$X(i)$	The ith particle position
$V(i)$	Velocity of the ith particle
$J(i)$	Current cost function value of the ith particle
$PB(i)$	Local optimal position of the ith particle
$BestS$	Global optimal location
$\omega(i)$	Inertia weight coefficient of iteration I
$c_1(i)$ *and* $c_2(i)$	Self and social learning factor
$T(i)$	Temperature
$P_i(k)$	The probability of the k-th iteration of the ith particle accepting the new solution
kg	Current evolutionary algebra
$P(i)$	Historical optimal extremum of the ith particle

$$X_i^{kg+1} = X_i^{kg} + V_i^{kg+1} \tag{7}$$

In particle swarm optimization algorithm, particles will keep approaching the optimal solution, but due to the speed and position update strategy of particles, particles are easy to fall into the vicinity of the local optimal solution, which makes it difficult for the algorithm to jump out of the local optimal solution. Based on the principle of solid-state annealing, simulated annealing algorithm generates new solutions through random disturbance, and accepts or rejects new solutions, which can jump out of the local optimal solution and find the global optimal solution in the search process. The combination of adaptive PSO and simulated annealing algorithm can improve the global search ability of the algorithm.

Based on the above description of simulated annealing strategy and PSO algorithm, the following SA-PSO algorithm flow can be obtained as Fig.4.

Adaptive Parameter Adjustment Strategy The key of particle swarm optimization is setting ω, c_1 and c_2. Compared with fixed parameters, adaptive parameter adjustment can change parameters continuously with the optimization process to better adapt to different optimization stages, so as to improve the performance and accuracy of the model.

Through adaptive parameter adjustment, the global search is preferred at the initial stage of iteration, and the local search is gradually preferred as the iteration proceeds. This paper uses hyperbolic tangent curve to control inertia weight coefficient ω and adopts the following adaptive parameter adjustment strategy:

$$\begin{aligned}\omega(i) = (\omega_{max} + \omega_{min})/2 + tanh(-4 + 8* \\ (G - i)/G) \cdot (\omega_{max} - \omega_{min})/2\end{aligned} \tag{8}$$

$$c_1(i) = c_{1max} - i(c_{1max} - c_{1min})/G \tag{9}$$

$$c_2(i) = c_{2min} + i(c_{2max} - c_{2min})/G \tag{10}$$

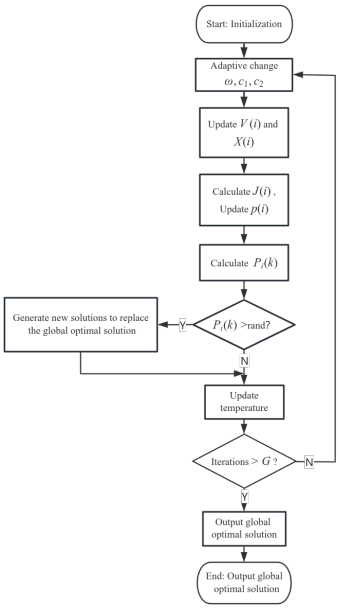

Fig. 4: SA-PSO algorithm flow

The basic parameters of adaptive parameter adjustment and the parameter settings based on references and experiments are shown in the Table 4.

Table 4: Parameters and Settings of Adaptive Parameter Adjustment

Range of inertia weight coefficient ω	[0.4,0.95]
Range of self learning factor c_1	[1.25,2.5]
Range of social learning factor c_2	[1.25,2.5]

At the beginning of the search, ω has larger value, $c_1 > c_2$, the algorithm tends to global search; With the generation selection, ω and the difference between c_1 and c_2 decreases gradually, and then $c_1 < c_2$, which makes the algorithm tend to local search.

3.3 Identification Results

Identification of Multi Frequency Signals Set the input signal amplitude to 1V and angular frequencies to 4, 6, 8, 12, and 16 (rad/s), respectively. Import the corresponding data to identify the physical model, record the identification effect diagram and error parameters. The vertical axis of the following image represents the voltage value (V), and the horizontal axis represents the time (s). The upward trend in the iteration curve is a visualization of the simulated annealing process.

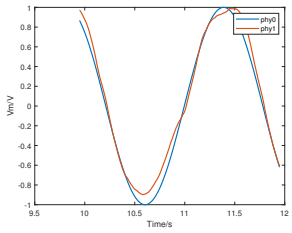

(a) ω=4rad/s

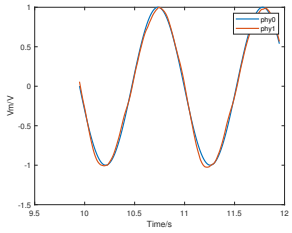

(b) ω=6rad/s

Fig. 5: Input signal and identification parameter fitting effect

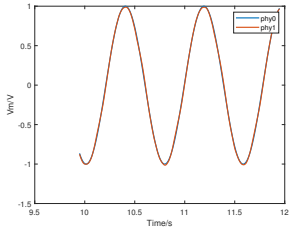

(a) ω=8rad/s

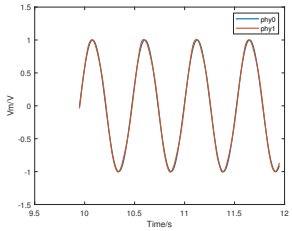

(b) ω=12rad/s

Fig. 6: Input signal and identification parameter fitting effect

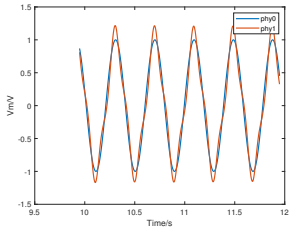

Fig. 7: Input signal and identification parameter fitting effect(ω=16rad/s)

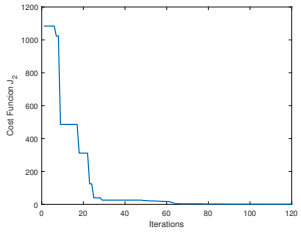

Fig. 8: Typical cost function variation diagram with amplitude of 1V and angular frequency of 8rad/s

In order to quantify the identification effect and its error, this article defines the percentage error of the model as the ratio of the root mean square error (RMSE) of the model to the absolute value of the average amplitude of the identification signal, which is given by the following formula:

$$e_k = \frac{RMSE}{A} = \frac{\sqrt{mse}}{A} \tag{11}$$

According to the graphs and Table 5, as the input signal frequency continues to increase, the identification effect shows a trend of first improving and then deteriorating. The simulation results show that the identification effect of the inverted pendulum system is optimal when the angular frequency is around 8 rad/s. At the same time, according to the cost function value variation graph, when the number of iterations reaches about 70, the sum of squared errors reaches less than 1.

Table 5: Identification Error Parameters for Input Signals with Different Angular Frequencies (Unit Omitted)

Input	J	R-square	e_k
$A = 1, \omega = 4$	8.6641	1.0033	9.31%
$A = 1, \omega = 6$	1.7419	0.9940	4.17%
$A = 1, \omega = 8$	0.2874	0.9974	1.69%
$A = 1, \omega = 12$	0.7190	1.0016	2.68%
$A = 1, \omega = 16$	18.0248	1.0312	13.43%

Based on the identification results at a relatively optimal identification frequency of 8 rad/s, the parameters of the physical model of the system can be obtained as shown in Table 6.

Table 6: Hardware System Parameters Based on MSSA-PSO Identification

a_1	a_2	a_3	a_4	a_5
4944	-9928	4985	-25	21
a_6	a_7	a_8	a_9	a_10
-43	43	-5087	10146	-5064

Effectiveness of Optimization Strategies In order to study the impact of optimization strategies such as Nonlinear Weight (NW), Adaptive Linear Learning (LL), and Simulated Annealing (SA) on system identification performance, the optimal input signal (amplitude 1V, angular frequency 8rad/s) was selected for the following simulation experiments. This article uses basic PSO algorithm, PSO algorithm of this article with removal of a certain optimization strategy, and multi strategy simulated annealing PSO algorithm (MSSA-PSO) to compare the convergence and accuracy of the algorithms. The author mainly compares the number of iterations (N) when the cost function value of system identification decreases to less than 1 and other identification error indicators.

Table 7: Convergence Speed and Error Indicators for System Identification Using Different Algorithms

Algorithm	N	J	R-square	e_k
PSO	> 200	9.1101	0.8677	9.54%
LLSA-PSO	> 200	7.7571	0.8815	8.81%
NWSA-PSO	136	0.4846	1.0025	2.20%
MS-PSO	> 200	1.0107	0.9754	3.18%
MSSA-PSO	125	0.1962	1.0002	1.40%

According to Table 7, both NWSA-PSO and MSSA-PSO can reach the convergence standard (N<1) within 150 iterations, and the identification effect is

splendid. The convergence rate of MSSA-PSO is the fastest and the percentage error is the smallest, which is less than 1.5%.
In order to further demonstrate the effectiveness of the algorithm design in this paper, we used this method and three algorithms to remove a certain strategy for the signal with a frequency of 8 rad/s for 20 independent repeated experiments, and drew the average iterative curve of 200 generations under the logarithmic coordinate log_{10} (J_2) (J_2 is the value of the surrogate function). It can be seen from figure 9 that the NW strategy and SA strategy have a great effect on improving the accuracy of the algorithm, while the LL strategy has little effect on the accuracy of the algorithm, but it can accelerate the convergence speed of the algorithm.

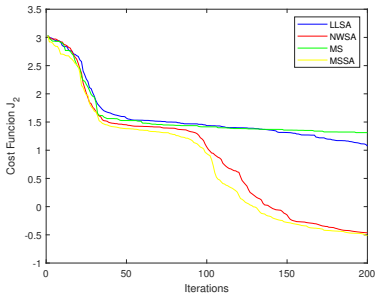

Fig. 9: Comparison of average iterative curve of algorithms

4 Explicit MPC Control

In order to verify that the identified model can be used to control the rotating inverted pendulum, we used the explicit MPC method to control the rotating inverted pendulum on the QUBE Servo 2 experimental equipment.

Explicit MPC was first proposed by Bemporad et al., which is an efficient method that is similar to the lookup table approach which can be used in embedded system or Real-time dynamic system when systems are under constraints. In this section, first we review the traditional MPC strategies . Then we introduce the explicit MPC method. Finally we represent the explicit MPC controller regulating effect on our identified system by PSO algorithm.

4.1 Model Predictive Control

Model Predictive Control (MPC) is able to handle constraints and multi-variable systems effectively by using receding horizon strategy. Consider that a discrete-time linear time invariant (LTI) system subjects to the following constraints:

$$x(k) \in \mathcal{X}, u(k) \in \mathcal{U} \tag{12}$$

where $x(k) \in \mathbb{R}^n$ is the state of system, $u(k) \in \mathbb{R}^m$ is the input of system and $y(k) \in \mathbb{R}^l$ is the output of system. $\mathcal{X}$ and $\mathcal{U}$ are the constraint sets of state and input, respectively.

The MPC optimization problem at time k can be formulated as:

$$\min_{u(k|k),\ldots,u(k+N-1|k)} \sum_{i=0}^{N-1} x^T(k+i+1)Qx(k+i+1) + u^T(k+i)Ru(k+i) \tag{13}$$

$$\text{s.t. } x(k+i+1|k) = Ax(k+i|k) + Bu(k+i|k)$$

where N is the prediction horizon, Q and R are positive semi-definite weighting matrices.

4.2 Explicit Model Predictive Control

The idea of explicite MPC is to beforehand solve the optimization problem (13) for all $x \in \mathcal{X}$. We wish to derive a division of $\mathcal{X}$ where we have explicit controller design formulation in all division ,which can be represented as

$$u(x) = \begin{cases} F_1 x + g_1 \text{ if } H_1 x \leq k_1 \\ \quad \vdots \quad \vdots \\ F_M x + g_M \text{ if } H_M x \leq k_M \end{cases} \tag{14}$$

By substituting $x(k+i|k) = A^i x(k) + \sum_{j=0}^{i-1} A^j B u(k+i-1-j)$, equation (13) can be rewritten as

$$V(x(k)) = \frac{1}{2}x^T(k)Yx(k) + \min_U \{\frac{1}{2}U^T HU + x^T(k)FU\} \tag{15}$$
$$\text{s.t.} \quad GU \leq W + Ex(k)$$

Define

$$z \triangleq U + H^{-1}F^T x(k) \tag{16}$$

Completing square in equation(15), we obtain the equivalent optimization problem

$$V_z(x(k)) = \min \frac{1}{2}z^T Hz \tag{17}$$
$$\text{s.t.} \quad Gz \leq W + Sx(k)$$

where $S \triangleq E + GH^{-1}F^T$ and $V_z(x(k)) = V(x(k)) - \frac{1}{2}x(k)^T(Y - FH^{-1}F^T)x(k)$.

Theorem2 in [18] has shown that when the rows of G are linearly independet. Let CR_0 be the set of all vectors x, for which such a combination is active at the optimun. Then the optimal z and the associated vector of Lagrange multipliers λ are uniquely defined affine functions of x over CR_0.

For Lagrange multipliers $\tilde{\lambda}$ corresponding to active constrains, $-\tilde{G}H^{-1}\tilde{G}^T\tilde{\lambda}-\tilde{W}-\tilde{S}x=0$,and therefore

$$\tilde{\lambda}=-(\tilde{G}H^{-1}\tilde{G}^T)^{-1}(\tilde{W}+\tilde{S}x) \tag{18}$$

$$z=H^{-1}\tilde{G}^T(\tilde{G}H^{-1}\tilde{G}^T)^{-1}(\tilde{W}+\tilde{S}x) \tag{19}$$

Note that z is an affine function of x.

4.3 Control Results

We employed the Explicit Multi-Parametric Solution provided by the YALMIP library to implement Explicit Model Predictive Control for the inverted pendulum system in MATLAB. To test the robustness of system, we apply a periodic pulse signal with an amplitude of 1V to the input port of the control system as disturbance, while the duty cycle of this pulse signal ranging from $5\% \sim 12\%$. The real-time Control parameter are setted as followed: The sample time $T_s = 0.002s$, the prediction horizon is selected as $N = 4$. Input voltage u subjects to $-10V \leq u \leq 10V$.

At inital time the derivative of θ and α are 0, so that we could derive the state-space partition of θ and α when $\dot{\theta}=0$ and $\dot{\alpha}=0$. Fig.10 and Fig.11 show optimizer and value function of w.r.t. θ and α at initial time.

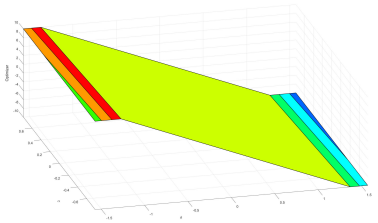

Fig. 10: Optimizer State-space partition

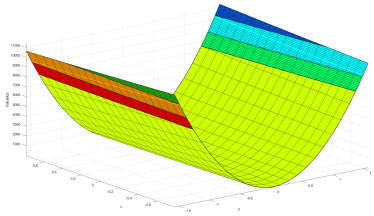

Fig. 11: Value Function State-space partition

Fig.10 shows how explicit mpc handles input constraints for $-10 \leq u \leq 10$ and Fig.11 is a Lyapunov function like value function which garentees the stability of this system.

In the disturbance experiments, we apply periodic pulse disturbances with duty cycles of 0.05, 0.08, 0.1, and 0.12 to the input port (the green curve in the figure on the left), and measure the corresponding system responses (the red curve (α) and blue curve(θ)) as shown in the following figures (12-15).
From Fig.(12-15), we can see that when a pulse disturbance is applied to the input, the system enters an uncontrolled state. During this time, the signal solved by eMPC is covered by the pulse disturbance, causing the system to rapidly deviate from the equilibrium state. After the pulse ends, the eMPC control input resumes.When the duty cycle is larger than 0.08, the input is constrained and limited to 10 by the MPC. The system's α and θ states rapidly recover to

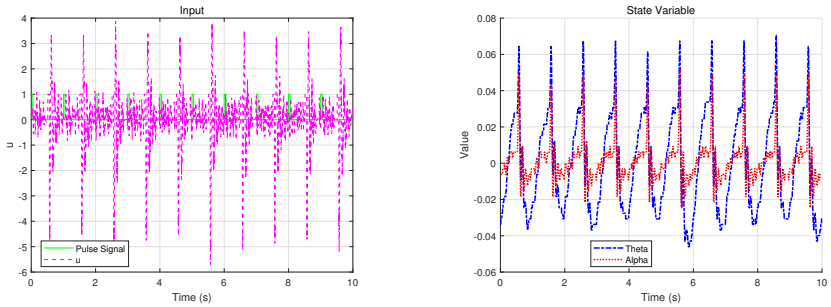

(a) Control input (b) System state quantity

Fig. 12: Control input and system state quantity under pulse disturbance with duty cycle of 0.05

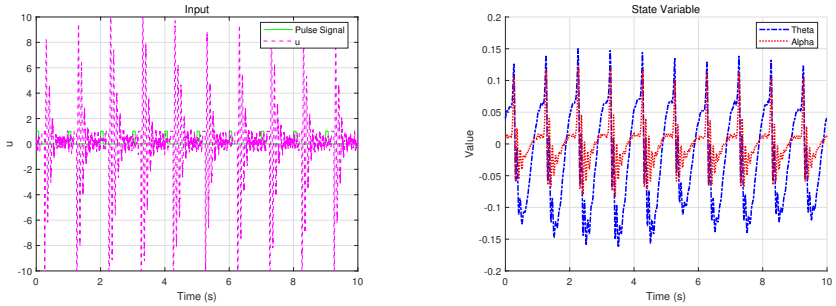

(a) Control input (b) System state quantity

Fig. 13: Control input and system state quantity under pulse disturbance with duty cycle of 0.08

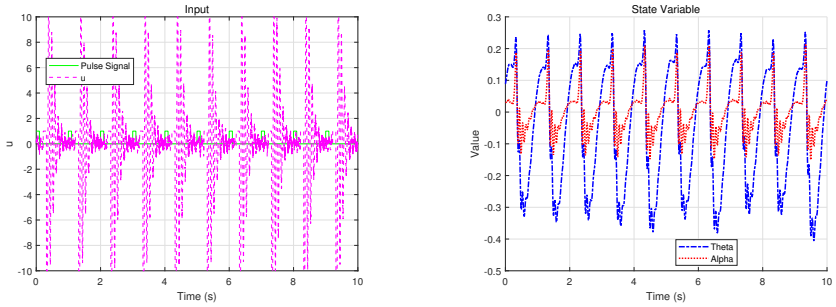

(a) Control input (b) System state quantity

Fig. 14: Control input and system state quantity under pulse disturbance with duty cycle of 0.10

equilibrium point 0 after the MPC solved signal is applied, indicating the system returns to a stable state.

To better illustrate the convergence region of our identified-based MPC, record the maximum deviation angle of α from which the system is still able

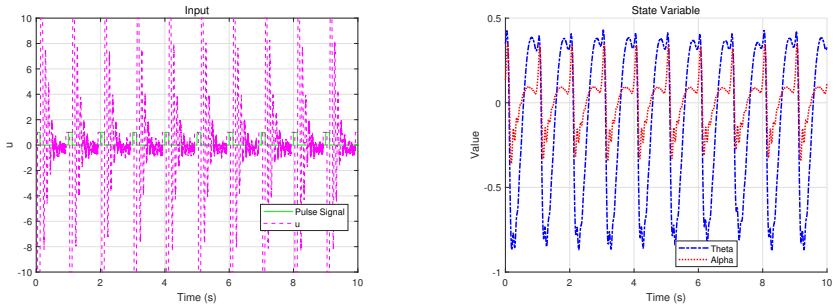

(a) Control input (b) System state quantity

Fig. 15: Control input and system state quantity under pulse disturbance with duty cycle of 0.12

to recover to the equilibrium state after the disturbance. Results are shown in Table 8.

Table 8: Angle variation range of α under different degrees of disturbance

Duty Cycle of Pulse	**Range of $\alpha(^o)$**
ρ=0.05	[-1.40, 2.99]
ρ=0.08	[-4.74, 6.88]
ρ=0.1	[-8.42, 11.97]
ρ=0.12	[-19.69, 19.34]

5 Conclusion

This article designs identification algorithms and control methods based on the QUBE motor inverted pendulum experimental platform.

A multi strategy optimized simulated annealing PSO algorithm (MSSA-PSO) is designed to achieve high-precision identification of the inverted pendulum system, and the relatively optimal identification signal frequency is given. Subsequently, based on the hardware system model identified by MSSA-PSO, this paper adopts a highly model dependent MPC method to stabilize the inverted pendulum, and solves the real-time problem of MPC by introducing the explicit MPC (eMPC) strategy. The pendulum has strong anti-interference ability while operating stably. Through the comprehensive design of identification control experiments, this paper verifies the feasibility and efficiency of the proposed identification model and corresponding control methods.

Acknowledgment

This work was supported in part by the National Natural Science Fund of China under Grant No.62207001.

References

1. Wang, JJ (Wang, Jia-Jun).Simulation studies of inverted pendulum based on PID controllers.[J].Simulation Modelling Practice and Theory,2011,Vol.19(1): 440-449.

2. Brett Ninness. Some System Identification Challenges and Approaches. IFAC Proceedings Volumes,42(10):1–20, 2009.
3. Jarrad Courts;Adrian Wills;Thomas Schön;Brett Ninness.Variational Nonlinear System Identification[J], 2020.
4. Wang,Yujue;Mao,Weining;Wang,Qing;Xin,Bin.Fuzzy Cooperative Control for the Stabilization of the Rotating Inverted Pendulum System[J].JOURNAL OF ADVANCED COMPUTATIONAL INTELLIGENCE AND INTELLIGENT INFORMATICS,2023,Vol.27(3): 360-371.
5. Fröhlich, Lukas.Data-Efficient Controller Tuning and Reinforcement Learning[D].2022.
6. Hao Xu;Jinhui Zhang;Hongjiu Yang;Yuanqing Xia.Extended State Functional Observer-Based Event-Driven Disturbance Rejection Control for Discrete-Time Systems[J].IEEE Transactions on Cybernetics,2022,Vol.52(7): 6949-6958.
7. Xuanchen Xiang;Ruisheng Diao;Shonda Bernadin;Simon Y. Foo;Fangyuan Sun;Ayodeji S. Ogundana.An Intelligent Parameter Identification Method of DFIG Systems Using Hybrid Particle Swarm Optimization and Reinforcement Learning[J].IEEE Access,2024,Vol.12: 44080-44090.
8. Eswari, Pasila;Ramalakshmanna, Y.;Durga Prasad, Ch.An Improved Particle Swarm Optimization-Based System Identification[J].Lecture Notes in Electrical Engineering,2021,Vol.749: 137-142.
9. Hazem Issa;József K. Tar.Improvement of an Adaptive Robot Control by Particle Swarm Optimization-Based Model Identification[J].Mathematics,2022,Vol.10(3609): 3609.
10. Jaouher Chrouta;Wael Chakchouk;Abderrahmen Zaafouri;Mohamed Jemli.Modeling, Identification and Control of Nonlinear System Based on Adaptive Particle Swarm Optimization[J].International Journal of Manufacturing Science and Technology,2018,Vol.12(1): 65-79.
11. Morteza Harati;Amir Aminzadeh Ghavifekr;Amir Rikhtehgar Ghiasi.Model Identification of Single Rotary Inverted Pendulum Using Modified Practical Swarm Optimization Algorithm[A].2020 28th Iranian Conference on Electrical Engineering (ICEE)[C],2020.
12. Bemporad, A., & Morari, M. (1999). Robust model predictive control: A survey. In A. Garulli, A. Tesi, & A. Vicino (Eds.), Robustness in identixcation and control, Lecture Notes in Control and Information Sciences Vol. 245 (pp. 207-226). Berlin: Springer.
13. Johannes Köhler;Matthas A. Müller;Frank Allgöwer.Analysis and design of model predictive control frameworks for dynamic operation – An overview[J].2023.
14. S. Yu, M. Hirche, Y. Huang, H. Chen, and F. Allgöwer, "Model predictive control for autonomous ground vehicles: A review," Auto. Intell. Syst., vol. 1, no. 1, pp. 1–17, Aug. 2021.
15. T. Gold, A. Völz, and K. Graichen, "Model predictive interaction control for industrial robots," IFAC-PapersOnLine, vol. 53, no. 2, pp. 9891–9898,2020.
16. Farrukh Waheed;Imran Khan;Michael Valášek.A TV-MPC Methodology for Uncertain Under-Actuated Systems: A Rotary Inverted Pendulum Case Study[J].IEEE Access,2023,Vol.11: 1.
17. Askari, Masood;Moghavvemi, Mahmoud;Almurib, Haider Abbas F.;Haidar, Ahmed M. A..Stability of soft-constrained finite horizon model predictive control[J].IEEE Transactions on Industry Applications,2017,Vol.53(6): 5883-5892.
18. Bemporad, A.*; Morari, M.; Dua, V.; Pistikopoulos, E.N..The explicit linear quadratic regulator for constrained systems[J].Automatica,2002,Vol.38(1): 3-20.